Computer Assisted Mechanics and Engineering Sciences, 8: 343–358, 2001.

T-element analysis of plates on unilateral elastic Winkler-type foundation

Jaroslav Jirousek
LSC-DGC, Swiss Federal Institute of Technology (EPFL), CH-1015 Lausanne, Switzerland

Andrzej P. Zieliński and Adam Wróblewski
Institute of Mechanics and Machine Design, Cracow University of Technology, al. Jana Pawła II 37, 30-864 Kraków, Poland

(Received June 30, 2000)

This paper presents a hybrid-Trefftz finite element algorithm designated as *fictitious load approach*. Its originality resides in the formulation and practical application of concepts which make it possible to account for the unilateral contact conditions of a plate without modification of the finite element mesh. To reach this aim, the approach allows the movable interface between the contact and non-contact parts of the plate to travers any finite element subdomain. The adjustments are confined to fictitious load dependent terms, while the element stiffness matrices remain unchanged during the whole iterative process. Several numerical examples are analysed to assess the effectivity of the T-element algorithm and to compare it with some of the existing solutions of the same problem.

Keywords: finite elements, Trefftz method, contact problem

1. Introduction

The solution of plates on unilateral elastic Winkler foundation is a highly non-linear contact problem since the non-contact pair of the lower surface of the plate is not known in advance. Its practical importance is due to fact that the unilateral nature of the support (capable to resist only the compression) may influence considerably the results.

The number of studies concerning the above problem is comparatively low and most of the contributions in this field come from the boundary element method (BEM) community of research workers [1, 2, 14, 16]. A solution combining the conventional finite element method (FEM) with a linear complementary equation approach based on the contact theory was also presented [4]. Moreover, a formulation using infinite series to represent the displacement profile was reported [18], but its practical usefulness is seriously compromised owing to its limitation to rectangular plates.

The aim of the present work is to study the opportunity of extending to the solution of the unilateral contact problem of plates on elastic Winkler foundation the so-called T-element approach. Initiated more than twenty years ago [5, 8] as a counterpart of the conventionally formulated (Ritz) finite elements (FE), this class of alternative FE formulations is based on a generalized form of the Trefftz method. As a consequence, the assumed displacement field is chosen so as to satisfy the governing differential equations of the problem. The boundary conditions and the interelement continuity of displacements and stresses are then enforced in the average integral sense.

In the past years many alternative T-element formulations were proposed (for a survey see [11, 13]), most of which fall into one of the two following categories:

- The hybrid formulations, in which the T-elements are linked through an auxiliary "frame" representing either the generalized displacement (the HT-D models) or the conjugate generalized boundary tractions (the HT-T models). They are defined on the element boundary in terms of nodal parameters, independently of the internal displacement field of the element.
- The direct formulations where the T-elements are linked without the help of any auxiliary boundary or interelement fields.

The most popular among these formulations is the basic hybrid-Trefftz displacement frame model. Such T-elements resemble externally the conventionally formulated h- or p-elements over which they have, however, several important advantages [7, 9–11, 13]: enhanced accuracy, fast p-convergence, facility of extending the p-element concept also to C^1 conformity problems, attractive possibility of library of optional special purpose T-functions for accurate solution of various singular or stress concentration problems without troublesome mesh refinement, calculation of local effects due to various arbitrary positioned concentrated and/or discontinuous loads without necessity of a mesh adjustment, simple and efficient p-adaptivity concept well suited for implementation into standard FE codes, etc.

The following three sections outline the theoretical formulation. The first of them (Section 2) is concerned with the solution of the governing differential 4th order equation with and without the Winkler foundation term and the generation of the corresponding T-complete displacement fields of the element. The second (Section 3) outlines some two T-element formulation for the plate on a bilateral Winkler foundation (the foundation sustains indifferently the compression and the tension, and the plate does not separate from its foundation in the case of upward deflection $w > 0$). The Section 4 extends the approach to an iterative solution of a contact problem which arises in presence of a unilateral Winkler foundation (contact area not known in advance) in which case the plate separates from its foundation if $w > 0$. All T-elements are of the p-method type and, as a consequence, the solution accuracy may be corrected by changing simply the optional number of the hierarchic DOF of the T-elements while keeping unchanged their mesh. Sections 5 and 6close this study with a short assessment and some concluding remarks.

In order to avoid cumbersome writing of some involved relations associated with various T-element formulations, use will be made, as much as possible, of a simplified matrix notation. Such notation is particularly useful for the definition of various T-element fields, such as for example the assumed displacement $w = w^e$ on the subdomain Ω^e of the element "e" (see (6)), or the generalized boundary displacements $\mathbf{v}$ and tractions $\mathbf{t}$ on the element boundary $\Gamma^e \equiv \partial\Omega^e$ (see (3.2), (3.2)). Hereafter will be admitted that

$$w = \mathring{w} + \mathbf{W}\mathbf{c} \qquad \text{on} \quad \Omega^e \tag{1}$$

and

$$\mathbf{v} = \mathring{\mathbf{v}} + \mathbf{V}\mathbf{c} \qquad \text{on} \quad \Gamma^e \tag{1a}$$

or

$$\mathbf{t} = \mathring{\mathbf{t}} + \mathbf{T}\mathbf{c} \qquad \text{on} \quad \Gamma^e, \tag{1b}$$

derived from w^e, are such that

$$w^e(\mathbf{x}^e) = \begin{cases} \mathring{w}^e(\mathbf{x}^e) + \mathbf{W}^e(\mathbf{x}^e)\mathbf{c}^e & \mathbf{x}^e \in \Omega^e \\ 0 & \mathbf{x}^e \notin \Omega^e \end{cases} \tag{2a}$$

and

$$\mathbf{v}^e(\mathbf{x}^e) = \begin{cases} \mathring{\mathbf{v}}^e(\mathbf{x}^e) + \mathbf{V}^e(\mathbf{x}^e)\mathbf{c}^e & \mathbf{x}^e \in \Gamma^e \\ 0 & \mathbf{x}^e \notin \Gamma^e \end{cases} \tag{2b}$$

or

$$\mathbf{t}^e(\mathbf{x}^e) = \begin{cases} \overset{\circ}{\mathbf{t}}{}^e(\mathbf{x}^e) + \mathbf{T}^e(\mathbf{x}^e)\mathbf{c}^e & \mathbf{x}^e \in \Gamma^e \\ 0 & \mathbf{x}^e \notin \Gamma^e. \end{cases} \tag{2c}$$

Further (Fig. 1) $\mathbf{x}^e = \{x^e, y^e\}^{\mathrm{T}}$ are the local Cartesian coordinates originated at the center of the element e.

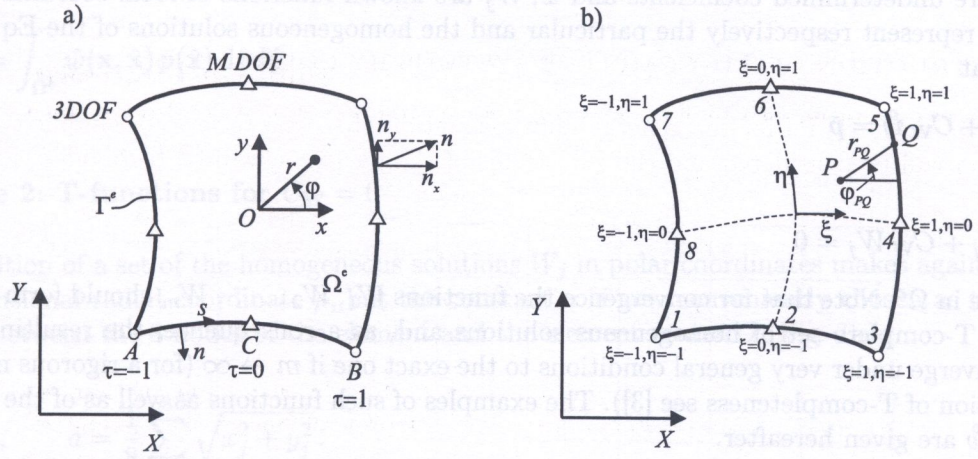

Fig. 1. Typical HT p-version of thin plate element: a) local Cartesian coordinates x, y and non-dimensional coordinate τ involved in evaluation of boundary integrals and in definition of element geometry; b) non-dimensional curvilinear coordinates ξ, η involved in evaluation of domain integrals and generation of internal control points

2. Solution of the governing differential equation

2.1. Governing differential equation

The analysis of the Kirchhoff plate on elastic Winkler foundation is governed by the well known 4th order partial differential equation

$$D\nabla^4 w + C_{\mathrm{W}}\, w = \bar{p}. \tag{3}$$

Here w and $\bar{p}$ stand for the transverse displacement and the given distributed load directed along the z axis (positive upward), $C_{\mathrm{W}} \geq 0$ designates the Winkler coefficient,

$$D = \frac{Eh^3}{12(1-\nu^2)}$$

is plate rigidity (E – Young's modulus, ν – Poisson's ratio, h – plate thickness) and ∇^4 stands for biharmonic operator, where

$$\nabla^2 = \frac{\partial^2}{\partial x^2} + \frac{\partial^2}{\partial y^2} = \frac{\partial^2}{\partial r^2} + \frac{1}{r}\frac{\partial}{\partial r} + \frac{1}{r^2}\frac{\partial^2}{\partial \varphi^2} \tag{4}$$

with $x = r\cos\varphi$, $y = r\sin\varphi$.

If the contact between the plate and the foundation is assumed to be unilateral (the soil foundation can bear compression only), the solution of Eq. (3) is physically meaningful only in the following two cases,

$$\begin{aligned} &\text{if } C_{\mathrm{W}} > 0 \quad \text{and} \quad w < 0, \\ &\text{if } C_{\mathrm{W}} = 0 \quad \text{and} \quad w \geq 0. \end{aligned} \tag{5}$$

The common feature of various HT-element formulations is the use of an assumed displacement field which satisfies the governing differential equation (3) *a priori* everywhere in the element subdomain Ω^e. Such field is of the form

$$w = \mathring{w} + \sum_{j=1}^{m} W_j c_j = \mathring{w} + \mathbf{W}\mathbf{c} \qquad \text{on } \Omega^e, \tag{6}$$

where c_j are undetermined coefficients and $\mathring{w}$, W_j are known functions of local coordinates x, y or r, φ which represent respectively the particular and the homogeneous solutions of the Eq. (3). This implies that

$$D\nabla^4 \mathring{w} + C_{\mathrm{W}} \mathring{w} = \bar{p} \tag{7}$$

and

$$D\nabla^4 W_j + C_{\mathrm{W}} W_j = 0 \tag{8}$$

everywhere in Ω^e. Note that for convergence the functions $W_1, W_2, \ldots, W_m$ should form a suitably truncated T-complete set of homogeneous solutions and, as a consequence, the resulting solution should converge under very general conditions to the exact one if $m \to \infty$ (for a rigorous mathematical definition of T-completeness see [3]). The examples of such functions as well as of the particular solutions $\mathring{w}$ are given hereafter.

2.2. Case 1: T-functions for $C_{\mathrm{w}} > 0$

The generation of the set of homogeneous solutions W_j in polar coordinates is simplified by the introduction of a non-dimensional radial coordinate

$$\rho = \frac{r}{a}, \qquad a = \sqrt{\frac{D}{C_{\mathrm{W}}}}. \tag{9}$$

This makes it possible to give the following simple explicit definition of the matrix $\mathbf{W} = \mathbf{W}(\rho, \varphi)$ of homogeneous solutions of the element,

$$\begin{aligned} \mathbf{W}(\rho,\varphi) = \big[& {}^{\mathrm{R}}f_0(\rho),\ {}^{\mathrm{I}}f_0(\rho) \big| , \\ & {}^{\mathrm{R}}f_1(\rho)\sin\varphi,\ {}^{\mathrm{I}}f_1(\rho)\sin\varphi,\ {}^{\mathrm{R}}f_1(\rho)\cos\varphi,\ {}^{\mathrm{I}}f_1(\rho)\cos\varphi \big| , \\ & {}^{\mathrm{R}}f_2(\rho)\sin 2\varphi,\ {}^{\mathrm{I}}f_2(\rho)\sin 2\varphi,\ {}^{\mathrm{R}}f_2(\rho)\cos 2\varphi,\ {}^{\mathrm{I}}f_2(\rho)\cos 2\varphi \big| \\ & \ldots \text{ etc. }] \end{aligned} \tag{10}$$

where

$${}^{\mathrm{R}}f_k(\rho) = \mathrm{Re} I_k(\rho\sqrt{\mathrm{i}}), \qquad {}^{\mathrm{I}}f_k(\rho) = \mathrm{Im} I_k(\rho\sqrt{\mathrm{i}}) \tag{11}$$

and where $I_k(\rho\sqrt{\mathrm{i}})$ designates the modified Bessel function with order k and $\mathrm{i} = \sqrt{-1}$.

Provided that the right hand side term in Eq. (3) is given in the Cartesian local coordinates, $\bar{p} = \bar{p}(x, y)$, as a polynomial of not more than 3rd degree, the particular term in (7) is simply

$$\mathring{w}(x, y) = \frac{1}{C_{\mathrm{W}}} \bar{p}(x, y). \tag{12}$$

In our case, however, $\bar{p}$ may be a function of a considerable complexity for which no such simple particular solution exists. Then the term $\mathring{w}$ may be evaluated by integrating the Green function

$$\hat{w}(\mathbf{x}, \hat{\mathbf{x}}) = -\frac{1}{4}\frac{a^2}{D} \mathrm{Re} H_0^{(1)}(\rho_{PQ}\sqrt{\mathrm{i}}) = -\frac{1}{4}\frac{a^2}{D}\, {}^{\mathrm{R}}g(\rho_{PQ}) \tag{13}$$

which stands here for the displacement at $\mathbf{x} = \mathbf{x}_Q$ (Fig. 1b) due to the point load $P = 1$ at $\hat{\mathbf{x}} = \mathbf{x}_P$. In the above, $H_0^{(1)}(\rho_{PQ}\sqrt{\mathrm{i}})$ stands for the Hankel function of the first kind with order zero and

$$\rho_{PQ} = \frac{r_{PQ}}{a}, \qquad r_{PQ} = \sqrt{(x-\hat{x})^2 + (y-\hat{y})^2}. \tag{14}$$

The application of the relation (13) makes it possible to write

$$\mathring{w}(\mathbf{x}) = \int_{\Omega^e} \hat{w}(\mathbf{x}, \hat{\mathbf{x}})\, \bar{p}(\hat{\mathbf{x}})\, \mathrm{d}\hat{x}\mathrm{d}\hat{y} \tag{15}$$

2.3. Case 2: T-functions for $C_{\mathrm{W}} = 0$

The definition of a set of the homogeneous solutions W_j in polar coordinates makes again use of the non-dimensional radial coordinate ρ, but the constant a is now conveniently chosen as the average distance between the 8 nodes of the element and the element center O (Fig. 1a):

$$\rho = \frac{r}{a}, \qquad a = \frac{1}{8}\sum_{j=1}^{8} \sqrt{x_j^2 + y_j^2}. \tag{16}$$

Unlike Case 1, the value of a may be different for each element and the use of a ρ close to 1 at the element boundary serves the purpose of avoiding numerical difficulties (overflow or underflow) arising for high values of the exponent of r encountered during the p-extension process.

The matrix $\mathbf{W}$ of homogeneous solutions may readily be generated in terms of increasing powers of non-domensionalized complex variable

$$\zeta = \frac{z}{a} = \frac{1}{a}(x + \mathrm{i}y) = \rho(\cos\varphi + \mathrm{i}\sin\varphi). \tag{17}$$

We obtain the following T-complete set of homogeneous solutions:

$$\begin{aligned}\mathbf{W}(\zeta) = [&1|, \mathrm{Re}\zeta\,, \mathrm{Im}\zeta\,|, \rho^2\,, \mathrm{Re}\zeta^2\,, \mathrm{Im}\zeta^2|,\\ &\rho^2\mathrm{Re}\zeta\,, \rho^2\mathrm{Im}\zeta\,, \mathrm{Re}\zeta^3\,, \mathrm{Im}\zeta^3|,\\ &\rho^2\mathrm{Re}\zeta^2,\ \rho^2\mathrm{Im}\zeta^2\,, \mathrm{Re}\zeta^4,\ \mathrm{Im}\zeta^4|,\\ &\ldots, \mathrm{etc.}]\,.\end{aligned} \tag{18}$$

The particular solution for a linearly distributed load is easy to obtain,

$$\bar{p} = \bar{p}_0 + \bar{p}_1 x + \bar{p}_2 y \quad \longrightarrow \quad \mathring{w} = \frac{1}{24}\, x^2 y^2 (3\bar{p}_0 + \bar{p}_1 x + \bar{p}_2 y). \tag{19}$$

As in Case 1 (see (15)), the particular solution for a more involved load distribution may be evaluated by integration of the Green function, now equal to

$$\hat{w}(\mathbf{x}, \hat{\mathbf{x}}) = \frac{\rho_{PQ}^2 \ln \rho_{PQ}^2}{16\pi D} \tag{20}$$

where ρ_{PQ} is defined by the relation (14).

3. T-ELEMENTS FOR PLATES ON WINKLER FOUNDATION

The formulations outlined in this section were obtained under the assumption that the Winkler foundation has the capability to sustain indifferently the compression (downward deflection; $w < 0$) and the tension (upward deflection, $w \geq 0$). As a consequence, the plate and the foundation show the same vertical displacements and do not separate as it is in the case of unilateral Winkler foundation (next Section) if the plate deflection $w > 0$.

In the following paragraphs of this section emphasis will be lain on the hybrid-Trefftz p-elements. Such elements resamble, externally, the conventionaly formulated conforming assumed displacement elements. This facilitates their application by the user and simplifies their implementation in the element library of any standard FE program.

3.1. Geometry of hybrid-Trefftz p-element

Figure 1 presents a typical quadrilateral HT plate bending p-element. Its theoretical formulation makes use of local Cartesian (x, y) and local polar (r, φ) coordinates originated at the element center O, conveniently defined in terms of global Cartesian coordinates (X, Y) of the eight element nodes (Fig. 1a) as

$$\mathbf{X}_O = \left\{ \begin{array}{c} X_0 \\ Y_0 \end{array} \right\} = \frac{1}{8} \sum_{j=1}^{8} \mathbf{X}_j \,. \tag{21}$$

With (21), the local Cartesian coordinates are simply

$$\mathbf{x} = \left\{ \begin{array}{c} x \\ y \end{array} \right\} = \mathbf{X} - \mathbf{X}_O \,. \tag{22}$$

The geometry of the particular element side $A{-}C{-}B$ (Fig. 1a) is quite general (straight, parabolic arc, circular arc, etc.) and is defined in a parametric form,

$$\mathbf{X}_{A-C-B}(\tau) = \left\{ \begin{array}{c} x_{A-C-B}(\tau) \\ y_{A-C-B}(\tau) \end{array} \right\}, \tag{23}$$

in terms of non-dimensional curvilinear coordinate τ varing from -1 to +1 between corner nodes A and B. The local notation A and B at the end point of a particular element side is chosen so that

$$N_A < N_B \tag{24}$$

where N_A and N_B stand for the global node numbers in the FE mesh. This rule warrants a unique definition of the positive sense of the coordinate τ ($\tau = \pm\xi$ or $\pm\eta$) as well as of s and n (Fig. 1a) along a side common to two neighbouring elements.

Whereas the element generation only involves the element boundary Γ^e, the iterative solution of the unilateral contact problem also involves calculations at control points and the integration over the element domain Ω^e. For this purpose it is convenient to express the local Cartesian coordinates of any point $x \in \Omega^e$ in terms of non-dimensional curvilinear coordinates ξ and η (Fig. 1b) varying from -1 to $+1$ between the opposite element sides.

3.2. Generalized boundary displacements and boundary tractions

All T-element formulations make use of suitably defined conjugate vectors of generalized boundary displacements $\mathbf{v}$ and boundary tractions $\mathbf{t}$. In the present study, these vectors will be defined as follows (Fig. 2):

$$\mathbf{v} = \left\{ \begin{array}{c} w \\ w_x \\ w_y \end{array} \right\} = \left\{ \begin{array}{c} w \\ \partial w/\partial x \\ \partial w/\partial y \end{array} \right\} = \left\{ \begin{array}{c} w \\ n_x w_n - n_y w_s \\ n_y w_n + n_x w_s \end{array} \right\} \tag{25}$$

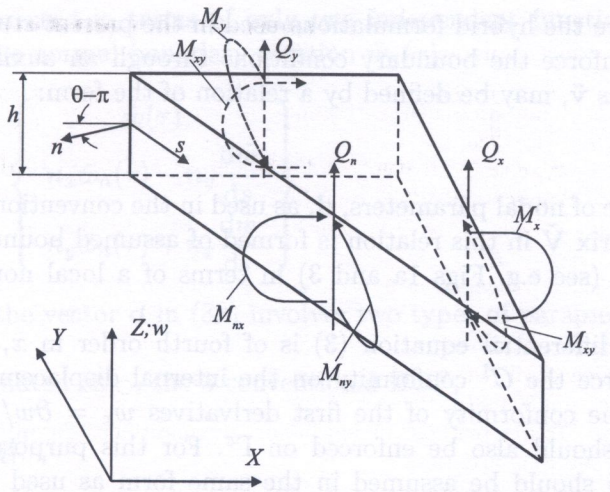

Fig. 2. Internal forces and generalized boundary tractions of a plate in bending

where $w_s = \dfrac{\partial w}{\partial s} = \dfrac{\partial \tau}{\partial s}\dfrac{\partial w}{\partial \tau}$, and

$$\mathbf{t} = \begin{Bmatrix} Q_n \\ -M_{nx} \\ -M_{ny} \end{Bmatrix} = \begin{Bmatrix} n_x Q_x + n_y Q_y \\ -n_x M_x - n_y M_{xy} \\ -n_y M_y - n_x M_{yx} \end{Bmatrix}. \tag{26}$$

Here

$$Q_x = -D\frac{\partial}{\partial x}\nabla^2 w, \tag{27}$$

$$Q_y = -D\frac{\partial}{\partial y}\nabla^2 w, \tag{28}$$

$$M_x = -D\left(\frac{\partial^2 w}{\partial x^2} + \nu\frac{\partial^2 w}{\partial y^2}\right), \tag{29}$$

$$M_y = -D\left(\frac{\partial^2 w}{\partial y^2} + \nu\frac{\partial^2 w}{\partial x^2}\right), \tag{30}$$

$$M_{xy} = -D(1-\nu)\frac{\partial^2 w}{\partial x \partial y}. \tag{31}$$

Finally n_x and n_y stand for components of the unit normal vector $\vec{n}$ (see Fig. 1 and 2) and the indexes n and s indicate in (25) the normal and tangential derivatives.

Should the element displacement field w be generated in polar coordinates then the Cartesian components of vector $\mathbf{v}$ (25) and $\mathbf{t}$ (26) can be evaluated more easily by an elementary transformation from the polar components w_r, w_φ, M_r, M_φ, $M_{r\varphi}$, Q_r, Q_φ.

Observing that the general form of the internal displacement field of the element (see (6)) is $w = \mathring{w} + \mathbf{Wc}$, and using the relation (25) and (26) leads to expressions (1a,b) namely $\mathbf{v} = \mathring{\mathbf{v}} + \mathbf{Vc}$ and $\mathbf{t} = \mathring{\mathbf{t}} + \mathbf{Tc}$, where $\mathring{\mathbf{v}}$, $\mathring{\mathbf{t}}$ and $\mathbf{Vc}$, $\mathbf{Tc}$ stand respectively for the particular and the homogeneous parts of the solution at the element boundary Γ^e.

3.3. Displacement frame

All hybrid T-element formulations make use of an auxiliary *frame function* defined at the element boundary Γ^e and representing either the generalized boundary displacements or the conjugate generalized boundary tractions [12, 13]. The T-element formulation with a *traction frame* is comparatively

complicated and therefore the hybrid formulations used in the present study (next subsection) will link the elements and enforce the boundary conditions through an auxiliary *displacement frame*. This frame, designated as $\tilde{\mathbf{v}}$, may be defined by a relation of the form:

$$\tilde{\mathbf{v}} = \tilde{\mathbf{V}}\mathbf{d} \quad \text{at } \Gamma^e \tag{32}$$

in terms of the same type of nodal parameters, $\mathbf{d}$, as used in the conventional assumed displacement finite elements. The matrix $\tilde{\mathbf{V}}$ in this relation is formed of assumed boundary functions $\tilde{V}_j$ defined along each element side (see e.g. Figs 1a and 3) in terms of a local non-dimensional curvilinear coordinate τ.

Since the governing differential equation (3) is of fourth order in x, y or ρ, φ, the T-element formulation should enforce the C^1 conformity on the internal displacement field w. This implies that for each element the conformity of the first derivatives $w_x = \partial w/\partial x$ and $w_y = \partial w/\partial y$, in addition to that of w, should also be enforced on Γ^e. For this purpose the components of the displacement frame (32) should be assumed in the same form as used in (25) for $\mathbf{v}$. Along the particular element side A–C–B (see Fig. 1a), the three components of $\tilde{\mathbf{v}}$, namely $\tilde{w}$, $\tilde{w}_x$ and $\tilde{w}_y$

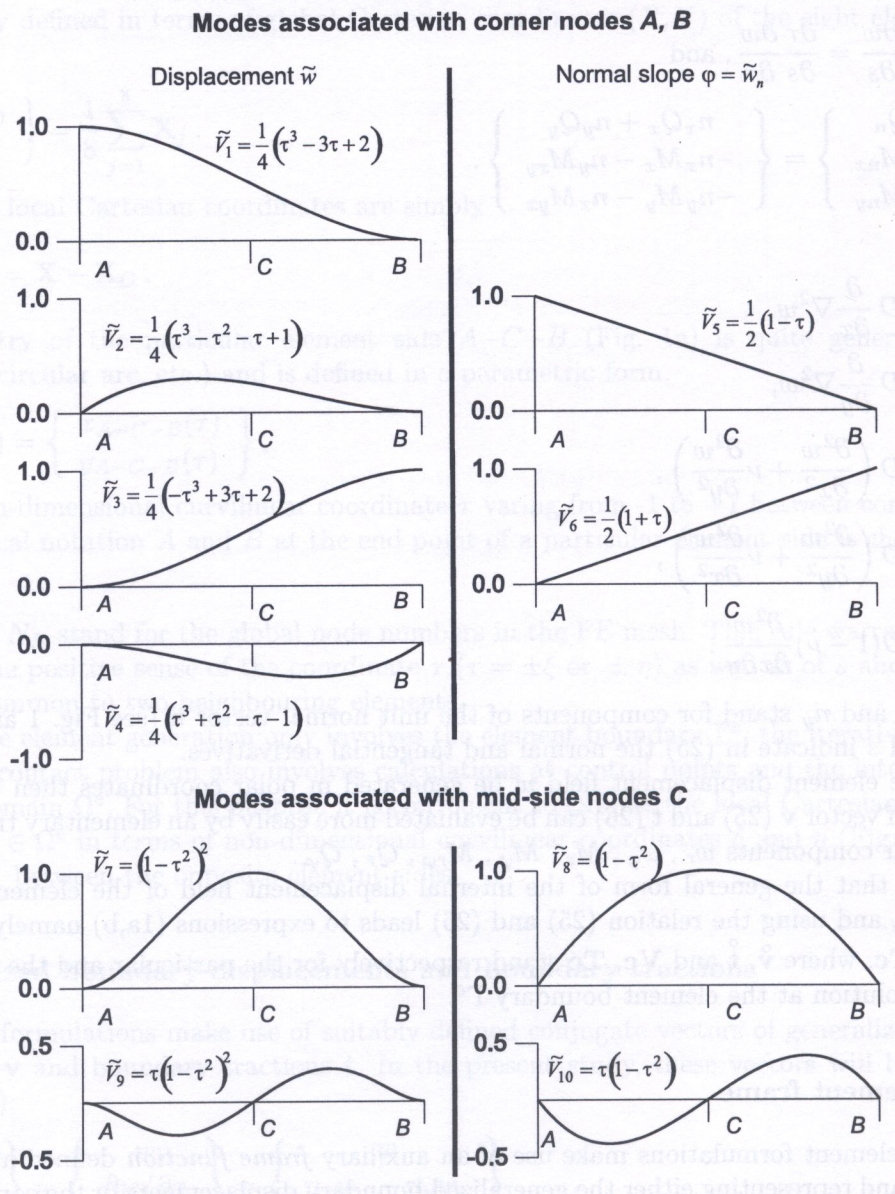

Fig. 3. Hierarchic displacement frame functions of the HT-D plate bending p-element

may conveniently be expressed in terms of only two independent functions of τ – the boundary displacement $\tilde{w}(\tau)$ and the normal boundary rotation $\tilde{w}_n(\tau)$:

$$\tilde{\mathbf{v}}(\tau) = \left\{ \begin{array}{c} \tilde{w}(\tau) \\ \tilde{w}_x(\tau) \\ \tilde{w}_y(\tau) \end{array} \right\} = \left\{ \begin{array}{c} \tilde{w}(\tau) \\ n_x \tilde{w}_n(\tau) - n_y \dfrac{\mathrm{d}\tilde{w}}{\mathrm{d}s} \\ n_y \tilde{w}_n(\tau) + n_x \dfrac{\mathrm{d}\tilde{w}}{\mathrm{d}s} \end{array} \right\}. \tag{33}$$

In the present study, the vector $\mathbf{d}$ in (32) involves two types of parameters (Fig. 1a):

- at corner nodes, designated as $\circ$, the 3 conventional DOF,

$$\begin{aligned} \mathbf{d}_A &= [\tilde{w}_A \ \tilde{w}_{xA} \ \tilde{w}_{yA}]^{\mathrm{T}}, \\ \mathbf{d}_B &= [\tilde{w}_B \ \tilde{w}_{xB} \ \tilde{w}_{yB}]^{\mathrm{T}}, \end{aligned} \tag{34}$$

- at the fictitious mid-side nodes $\triangle$, an optional number, M, of hierarchic side-mode DOF

$$\mathbf{d}_C = \left[{}^1\Delta\tilde{w}_{nC} \ {}^1\Delta\tilde{w}_C \ {}^2\Delta\tilde{w}_{nC} \ {}^2\Delta\tilde{w}_C \ \ldots \text{ etc.} \right]^{\mathrm{T}} \tag{35}$$

with the shape functions $\tilde{V}_j = \tilde{V}_j(\tau)$ $(j = 1, 2, \ldots)$ displayed in Fig. 3 and with

$$\begin{aligned} \tilde{w}_{\tau A} &= |\mathbf{s}_A| \, (-n_y \tilde{w}_{xA} + n_x \tilde{w}_{yA}), \\ \tilde{w}_{\tau B} &= |\mathbf{s}_B| \, (n_y \tilde{w}_{xB} + n_x \tilde{w}_{yB}), \end{aligned} \tag{36}$$

where $|\mathbf{s}_A|$, $|\mathbf{s}_B|$ stand for modulae of tangent vectors $\mathbf{s}_A$, $\mathbf{s}_B$, and

$$\begin{aligned} \tilde{w}_{nA} &= n_{xA} \tilde{w}_{xA} + n_{yA} \tilde{w}_{yA}, \\ \tilde{w}_{nB} &= n_{xB} \tilde{w}_{xB} + n_{yB} \tilde{w}_{yB}. \end{aligned} \tag{37}$$

The independent functions $\tilde{w}(\tau)$ and $\tilde{w}_n(\tau)$ along particular side $A{-}C{-}B$ of the element have the following definitions,

$$\tilde{w}(\tau) = \tilde{V}_1(\tau)\tilde{w}_A + \tilde{V}_2(\tau)\tilde{w}_{\tau A} + \tilde{V}_3(\tau)\tilde{w}_B + \tilde{V}_4(\tau)\tilde{w}_{\tau B} + \sum_{k=1,2,\ldots} \tilde{V}_{2k+5}(\tau) \, {}^k\Delta\tilde{w}_C, \tag{38}$$

$$\tilde{w}_n(\tau) = \tilde{V}_5(\tau)\tilde{w}_{nA} + \tilde{V}_6(\tau)\tilde{w}_{nB} + \sum_{k=1,2,\ldots} \tilde{V}_{2k+6}(\tau) \, {}^k\Delta\tilde{w}_{nC}. \tag{39}$$

3.4. Hybrid T-element formulation

The application of the internal displacement field $w = \mathring{w} + \mathbf{W}\mathbf{c}$ involving appropriate T-functions ($\mathring{w}$ and W_j) from Section 2 and linking the elements through the independly assumed generalized boundary displacements $\tilde{\mathbf{v}} = \tilde{\mathbf{V}}\mathbf{d}$ (32) leads in all hybrid formulations to a force–displacement relationship of the form

$$\mathbf{r} = \mathring{\mathbf{r}} + \mathbf{k}\mathbf{d}. \tag{40}$$

Here $\mathbf{r}$ stands for the vector of generalized nodal forces conjugate to $\mathbf{d}$, $\mathring{\mathbf{r}}$ is the part of $\mathbf{r}$ due to the particular solution $\mathring{w}$ and/or to imposed boundary tractions $\bar{\mathbf{t}}$ (if prescribed at Γ^e) and $\mathbf{k}$ is the element stiffness matrix.

The formulation based on the concept of *opposite weights* (HT-D elements) is defined by the following two weighted residual statements:

$$\int_{\Gamma^e} \delta \mathbf{t}^{\mathrm{T}} (\mathbf{v} - \tilde{\mathbf{v}}) \, \mathrm{d}\Gamma = 0 , \tag{41}$$

$$\int_{\Gamma^e} \delta \tilde{\mathbf{v}}^{\mathrm{T}} \mathbf{t} \, \mathrm{d}\Gamma = \int_{\Gamma_t^e} \delta \tilde{\mathbf{v}}^{\mathrm{T}} \bar{\mathbf{t}} \, \mathrm{d}\Gamma + \delta \mathbf{d}^{\mathrm{T}} \mathbf{r} . \tag{42}$$

With $\mathbf{v} = \overset{\circ}{\mathbf{v}} + \mathbf{V}\mathbf{c}$, $\mathbf{t} = \overset{\circ}{\mathbf{t}} + \mathbf{T}\mathbf{c}$ and $\tilde{\mathbf{v}} = \tilde{V} d$, this formulation leads to

$$\begin{aligned} \mathbf{c} &= -\mathbf{H}^{-1}\mathbf{g} + \mathbf{H}^{-1}\mathbf{G}\mathbf{d} , \\ \overset{\circ}{\mathbf{r}} &= \mathbf{h} - \mathbf{G}^{\mathrm{T}}\mathbf{H}^{-1}\mathbf{g} , \\ \mathbf{k} &= \mathbf{G}^{\mathrm{T}}\mathbf{H}^{-1}\mathbf{G} , \end{aligned} \tag{43}$$

where

$$\begin{aligned} \mathbf{g} &= \int_{\Gamma^e} \mathbf{T}^{\mathrm{T}} \overset{\circ}{\mathbf{v}} \, \mathrm{d}\Gamma , & \mathbf{h} &= \int_{\Gamma^e} \tilde{\mathbf{V}}^{\mathrm{T}} \overset{\circ}{\mathbf{t}} \, \mathrm{d}\Gamma - \int_{\Gamma_t^e} \tilde{\mathbf{V}}^{\mathrm{T}} \bar{\mathbf{t}} \, \mathrm{d}\Gamma , \\ \mathbf{H} &= \int_{\Gamma^e} \mathbf{T}^{\mathrm{T}} \mathbf{V} \, \mathrm{d}\Gamma = \int_{\Gamma^e} \mathbf{V}^{\mathrm{T}} \mathbf{T} \, \mathrm{d}\Gamma , & \mathbf{G} &= \int_{\Gamma^e} \mathbf{T}^{\mathrm{T}} \tilde{\mathbf{V}} \, \mathrm{d}\Gamma . \end{aligned} \tag{44}$$

Note that $\mathbf{H}$ is a symmetric positive definite matrix.

4. Plates on unilateral Winkler foundation — the fictitious load scheme

4.1. Two iterative approaches

The interaction between the plate and the unilateral Winkler foundation is a typical contact problem in which the frontier of the contact area (part of whole plate where $w \leq 0$) is not known in advance. To solve this problem, an iterative approach, of which several possibilities exist, should be used.

4.1.1. First approach

This approach is obtained if one converts the equation

$$D\nabla^4 w + C_{\mathrm{W}} w = \bar{p} \tag{45}$$

into the following iterative form,

$$(D\nabla^4 + C_{\mathrm{W}})\, {}^{i}w = {}^{i}p, \tag{46}$$

$${}^{i}p = \begin{cases} \bar{p} & \text{if } {}^{i-1}w \leq 0, \\ \bar{p} + C_{\mathrm{W}}\, {}^{i-1}w & \text{if } {}^{i-1}w > 0, \end{cases} \tag{47}$$

where $i = 1, 2, \ldots$ and ${}^{0}p = \bar{p}$. Here the homogeneous part of the solution is represented by the set of T-functions (10) and the particular solution ${}^{i}\overset{\circ}{w}$ due to the right hand side ${}^{i}p$ may be evaluated at the element sub-domain Ω^e as

$${}^{i}\overset{\circ}{w}(x) = \int_{\Omega^e} \hat{w}(\mathbf{x}, \hat{\mathbf{x}})\, {}^{i}p(\hat{\mathbf{x}}) \, \mathrm{d}\hat{x}\mathrm{d}\hat{y} \qquad (\hat{x}, \hat{y}) \in \Omega^e , \tag{48}$$

where $\hat{w}(\mathbf{x}, \hat{\mathbf{x}})$ is defined by Eq. (13). It is worthwhile to observe that when Eqs. (46)–(48) are used, the contact or not contact situation can change from one point to another inside one element.

4.1.2. Second approach

An alternative approach is generated if one realizes that instead of Eqs. (46) to (47) Eq. (45) can also be trasformed into

$$D\nabla^4 {}^i w = {}^i p, \tag{49}$$

$${}^i p = \begin{cases} \bar{p} & \text{if } {}^{i-1}w \geq 0, \\ \bar{p} - C_{\mathrm{W}}\, {}^{i-1}w & \text{if } {}^{i-1}w < 0. \end{cases} \tag{50}$$

The iterative process will be similar but now with the biharmonic functions (Sec. 2.3).

4.2. Additional considerations

Equations (46)–(48) or (49)–(50) suggest that stiffness matrices $\mathbf{k}^e$ $(e = 1, 2, \ldots, n_k)$ and the assembled stiffnes matrix $\mathbf{K}$ (of the whole structure) remain unchanged during the whole iterative process and the evolution of the contact/non-contact situation will only be controlled by successive modifications of the fictitious load component. This situation is reflected at the element level in the force–displacement relationship of the form

$${}^i\mathbf{r}^e = {}^i\mathring{\mathbf{r}}^e + \mathbf{k}^e {}^i\mathbf{d}^e, \tag{51}$$

the customary assembly process of which results at the level of the whole structure into a system of linear equations with a symmetric positive-definite coefficient matrix.

Thanks to the absence in the set (10) of T-functions to any rigid body motion modes suspectible of complicating the application of the 'opposite weights' form of the weighted residual method (vanishing of boundary tractions corresponding to these modes), the development of the element matrices may be based on the standard HT-D formulation (Sec. 3.4), the simplest and most inexpensive T-element form to be known.

The initial solution $(i = 0)$ is based on the assumption that the contact between the plate and the foundation extends over the whole FE mesh ($w \leq 0$ everywhere in $\Omega = \bigcup_e \Omega^e$). Provided that the above assumption does not hold true, the solution in the subsequent cycles $(i = 1, 2, \ldots)$ is then iteratively adjusted via the fictitious distributed load with intensity of $C_{\mathrm{W}}\, {}^{i-1}w_k^e$ at all control points where ${}^{i-1}w > 0$. This leads to solving the system of equations with still the same matrix $\mathbf{K}$ (the stiffness matrix of the assembly of elements) for a new right hand side ${}^i\mathring{\mathbf{R}}$. Provided that this process converges, the solution is terminated if the relative percentage error

$$\varepsilon\% = \frac{\max \left| {}^i w_k^e - {}^{i-1}w_k^e \right|}{\max \left| {}^i w_k^e \right|} \times 100\%, \qquad (e = 1, 2, \ldots, n_e; \quad k = 1, 2, \ldots, n_k) \tag{52}$$

does not exceed the specified allowable value.

4.3. Implementation

Since the approach outlined in the preceding paragraph does not need any iterative modification of the initial $(0 = 1)$ FE mesh, its implementation into most of the existing FE codes is easy. Provided that such codes (such as e.g. the program SAFE [6]) have the capability of solving sequentially any number of independent second members, then basically the only difference resides in their specification. While, normally, they are read from the INPUT file, now they are generated, for $i > 0$, directly by the program.

To facilitate the implementation, the flowchart displayed in Fig. 4 is helpful in the understanding and the organization of the calculations. Note that the effects of the given load alone (no fictitious loads) as obtained in the initial cycle $i = 0$ is calculated only once and need not be recalculated in subsequent cycles $i = 1, 2, \ldots$

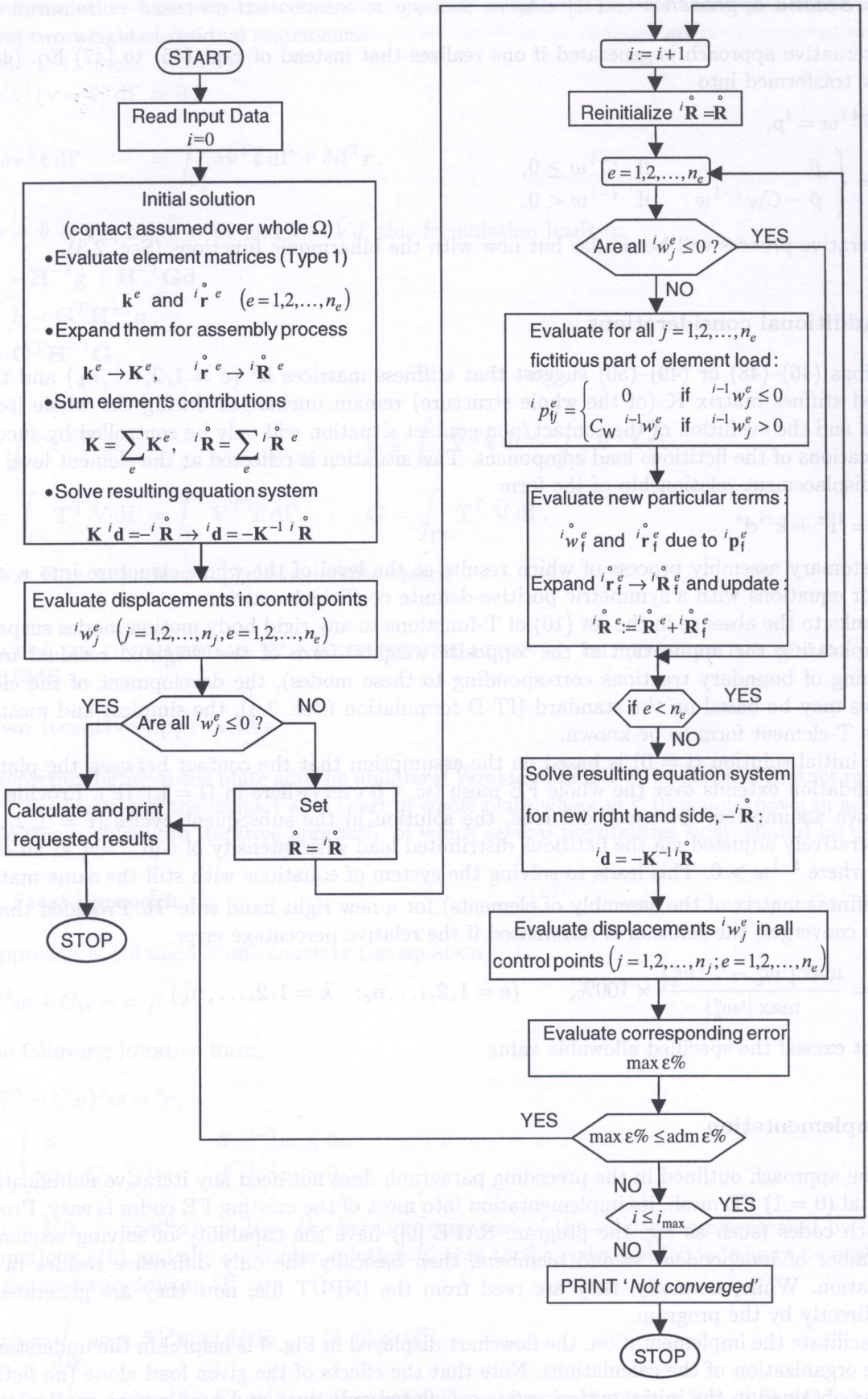

Fig. 4. Implementation of the first iterative approach

5. NUMERICAL ASSESSMENT

While the preceding theoretical developments concerned the HT p-version elements, the numerical assessment presented in this section will be confined to a single member of this family. Unless stated otherwise, this member represents a quadrilateral curve-side element with 3 DOF at corner nodes and 1 DOF at mid-side nodes. The results of this study will include the number of iterations which is needed for achieving the required accuracy.

Example 1: Long beam on unilateral Winkler foundation

As the first numerical example the authors have chosen a long beam ($L = 4.0$ [m]) with a rectangular ($b \times h$) cross-section, which is analogous to a plate subjected to cylindrical deformations. The beam was loaded in its center by a concentrated force $P = 10$ [kN]. It was characteristic, that the limit contact points depended here only on the material and geometrical data and not the value of the force. One can derive the analytical expression for the length L^c of the contact zone,

$$L^c \equiv L^c_{EX} = \frac{\pi}{2\lambda}, \qquad \text{where} \quad \lambda = \frac{C_W b}{4EI}. \tag{53}$$

For $E = 210$ [GPa], $C_W = 90$ [MPa/m], $b = 0.01$ [m] and $h = 0.3$ [m], we obtained therefrom $L^c = 3.362596$ [m]. Shorter beams are obviously in full contact with the foundation along their whole length.

Figure 5 presents in the logarithmic scale the absolute value of the error

$$\text{Error} = \frac{L^c_{NUM} - L^c_{EX}}{L^c_{EX}} \tag{54}$$

versus the number of the Gaussian points in the element of the beam. The increase of this number above $N_{GP} = 8$ appeared to be unprofitable. In the elements loosing their contact with the foundation the fictitious compensatory forces were here applied according to the algorithm defined by Eqs. (46)–(48).

Figure 6 compares efficiency of the two alternative algorithms — Eqs. (46)–(47) and (49)–(50) of the Sec. 4.1. As one can observe, both give similar results, but the second one needs much more

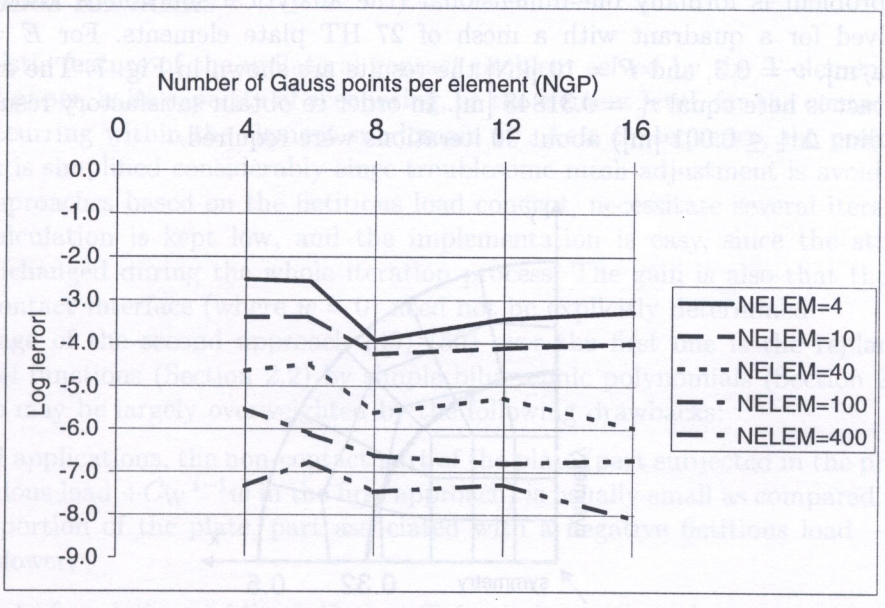

Fig. 5. Long beam on unilateral Winkler foundation. Error in location of limit contact point for number of elements NELEM, and for different number of Gauss points per element NGP. (1st approach — see Section 4.1.1)

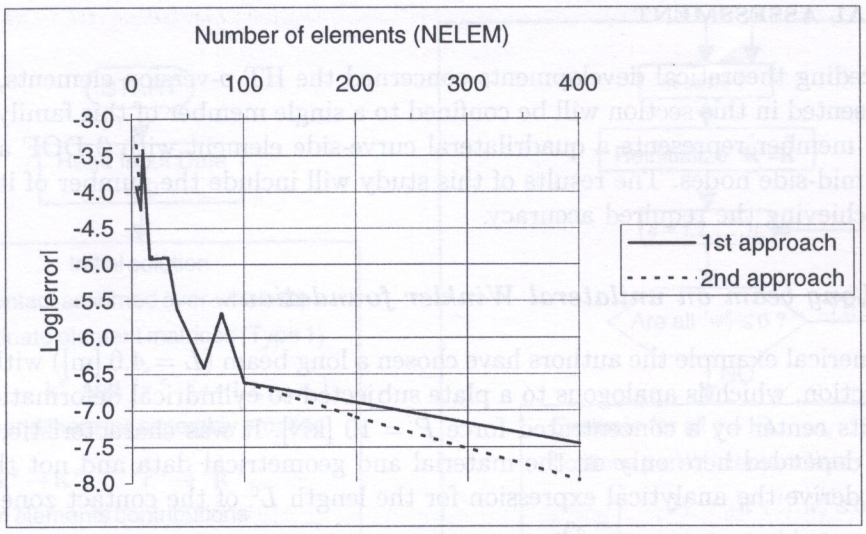

Fig. 6. Long beam on unilateral Winkler foundation. Comparison of two iteration algorithms: 1st approach (Section 4.1.1) with 20–30 iterations; 2nd approach (Section 4.1.2) with 90–110 iterations

iterations. It calls for some comments. The standard beam element has three rigid body modes and hence, for beam structure, one has to fix at least three degrees of freedom. In the above example we know nothing about the beam deflection, and the beam slope can be determined only at the point $x = 0$. To solve the problem we formally enforce the deflection at the point $x = 0$ instead of applying the force. The value of such deflection is determined in the additional iteration process with the condition that the sum (in the integral sense) of foundation reaction is equal to the applied force. It should be mentioned that such a problem exists only for the beams without displacement conditions.

Example 2: Circular plate on unilateral Winkler foundation

In the next example was investigated a circular plate subjected to a concentrated load P in the middle. This problem is formally one-dimensional (the analytical solution is known (see [17])), but it was solved for a quadrant with a mesh of 27 HT plate elements. For $E = 210$ [GPa], $C_W = 90$ [MPa/m], $\nu = 0.3$, and $P = 10$ [kN] the results are shown in Fig. 7. The exact radius of the loss of contact is here equal $r_c = 0.31848$ [m]. In order to obtain satisfactory results (difference in length of radius $\Delta r_c \leq 0.001$ [m]) about 30 iterations were required.

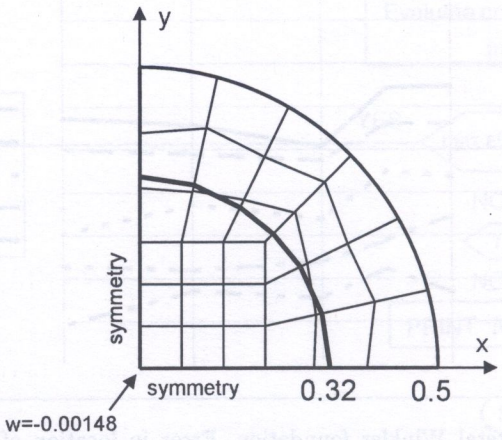

Fig. 7. Circular plate on unilateral Winkler foundation; thick line stands for separation between contact and non-contact zones

Example 3: Rectangular plate on unilateral Winkler foundation

The last example presents deformations of a rectangular plate loaded continuously on a central square (Fig. 8, [15]). Here $E = 23$ [GPa], $\nu = 0.17$, $C_W = 20$ [MPa/m], the load $q = 2$ [MPa] and $a \times b \times h = 9.6\,[\mathrm{m}] \times 7.2\,[\mathrm{m}] \times 0.2\,[\mathrm{m}]$ – the dimensions of the plate. For both, the 3×4 mesh of HT large elements and the standard ANSYS finite elements (small squares, dashed lines) the results were fairly close, with the accuracy to the thickness of the diagram line.

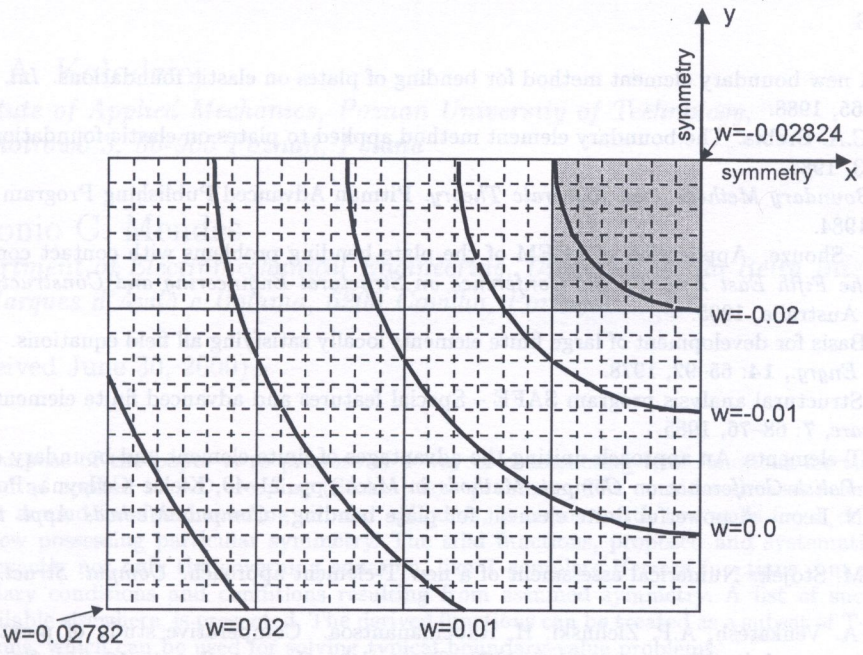

Fig. 8. Rectangular plate subjected to continuous load (shaded area), zones of constant deflection ($w > 0$ – loss of contact)

6. Concluding remarks

The characteristic feature of the unilateral contact problem solved by the T-element approach, as studied in this paper, is its capacity of accounting, at the element level, for the contact/non-contact phenomena occurring within the element subdomain Ω^e. As a consequence, the programmer's and analyst's work is simplified considerably since troublesome mesh adjustment is avoided.

The two approaches based on the fictitious load concept, necessitate several iterations, but the cost of the calculation is kept low, and the implementation is easy, since the stiffness properties remain unchanged during the whole iteration process. The gain is also that the intraelement contact/non-contact interface (where $w = 0$) need not be explicitly determined.

An advantage of the second approach (49)–(50) over the first one is the replacement of the modified Bessel functions (Section 2.2) by simple biharmonic polynomials (Section 2.3). However, this advantage may be largely overweighted by the following drawbacks:

- In practical applications, the non-contact part of the plate (part subjected in the present solution to the fictitious load $+C_W{}^{i-1}w$ in the first approach) is usually small as compared with the large remaining portion of the plate, part associated with a negative fictitious load $-C_W{}^{i-1}w$ and converges slower;

- If the plate to foundation rigidity ratio is sufficiently large, then the contact between the plate and its foundation is maintained over the whole domain. In the first of the presented approaches this solution is accurately represented already by the initial solution — the $i = 1$ step.

ACKNOWLEDGEMENT

Grant KBN PB 537/T11/97/13 is acknowledged. Also, the first author gratefully acknowledges the lasting support of LSC (Prof. F. Frey) which provided him with free access to various research facilities and thus made possible the continuation of his scientific activity while being officially retired.

REFERENCES

[1] G. Bezine. A new boundary element method for bending of plates on elastic foundations. *Int. J. Solids Struct.*, **24**(6): 556–565, 1988.

[2] J.A. Costa, C.A. Brebia. The boundary element method applied to plates on elastic foundations. *Engng. Anal.*, **2**(4): 174–183, 1985.

[3] I. Herrera. *Boundary Methods – an Algebraic Theory.* Pitman Advanced Publishing Program, Boston-London-Melbourne, 1984.

[4] X. Jiarun, X. Shouze. Application of LCEM of the plate bending problems with contact conditions. In: *Proceedings of the Fifth East Asia–Pacific Conference on Structural Engineering and Construction*, pp. 139–144, Queensland, Australia, 1995.

[5] J. Jirousek. Basis for development of large finite elements locally satisfying all field equations. *Comput. Methods Appl. Mech. Engrg.*, **14**: 65–92, 1978.

[6] J. Jirousek. Structural analysis program SAFE – Special features and advanced finite element models. *Adv. in Engng Software*, **7**: 68–76, 1985.

[7] J. Jirousek. T-elements: An approach uniting the advantages of finite element and boundary element methods. In: *Proc. XI Polish Conference on Comput. Methods in Mech.*, pp. 21–40, Kielce–Cedzyna, Poland, 1993.

[8] J. Jirousek, N. Leon. A powerful finite element for plate bending. *Comput. Methods Appl. Mech. Engrg.*, **12**: 77–96, 1977.

[9] J. Jirousek, M. Stojek. Numerical assessment of a new T-element approach. *Comput. Struct.*, **57**(3): 367–378, 1995.

[10] J. Jirousek, A. Venkatesh, A.P. Zieliński, H. Rabemanantsoa. Comperative study of p-extensions based on conventional assumed displacement and hybrid-Trefftz models. *Comput. Struct.*, **46**: 261–278, 1993.

[11] J. Jirousek, A. Wróblewski. T-elements: State of the art and future trends. *Arch. Comput. Meth. Engng*, **8**(4), 1996.

[12] J. Jirousek, A.P. Zieliński. Study of two complementary hybrid-Trefftz p-element formulations. In: C. Hirsch, O.C. Zienkiewicz, E. Oñate, eds., *Numerical Methods in Engineering '92, Proc. First European Conf. on Numer. Methods in Engng*, pp. 583–590, Brussels, 1992. Elsevier.

[13] J. Jirousek, A.P. Zieliński. Survey of Trefftz-type element formulations. *Comput. Struct.*, **63**: 225–242, 1997.

[14] J.T. Katsikadelis et al. Plates on elastic foundation by B.I.E. methods. *J. Engng. Mech.*, **110**(7): 1086–1105, 1984.

[15] R. Lewandowski, R. Świtka. Unilateral plate contact with the elastic-plastic Winkler-type foundation. *Comput. Struct.*, **39**(6): 641–651, 1991

[16] J. Puttonen, P. Varpasuo. Boundary element analysis of a plate on elastic foundations. *Int. J. Numer. Methods Engng*, **23**: 287–303, 1984.

[17] S. Timoshenko, S. Woinowsky-Krieger. *Theory of Plates and Shells.* McGraw–Hill Book Company, Inc., New York–Toronto–London, 1959

[18] B. Xiaoming, Y. Zhongda. Bending problems of rectangular thin plate with free edges laid on tensionless Winkler foundation. *Appl. Math. Mech.*, **10**(5): 435–442, 1989.